Communications between the High-Affinity Cyclic Nucleotide Binding Sites in E. coli Cyclic AMP Receptor Protein: Effect of Single Site Mutations †

ARTICLE *in* BIOCHEMISTRY · NOVEMBER 2002

Impact Factor: 3.02 · DOI: 10.1021/bi026099z · Source: PubMed

Communications between the High-Affinity Cyclic Nucleotide Binding Sites in *E. coli* Cyclic AMP Receptor Protein: Effect of Single Site Mutations†

Shwu-Hwa Lin and J. Ching Lee*

Department of Human Biologic Chemistry and Genetics, The University of Texas Medical Branch at Galveston, Galveston, Texas 77555-1055

Received May 8, 2002; Revised Manuscript Received July 10, 2002

ABSTRACT: The binding of adenosine 3′,5′-cyclic monophosphate (cAMP) and its nonfunctional analogue, guanosine 3′,5′-cyclic monophosphate (cGMP), to the adenosine 3′,5′-cyclic monophosphate receptor protein (CRP) from *Escherichia coli* was investigated by means of fluorescence and isothermal titration calorimetry (ITC) at pH 7.8 and 25 °C. A biphasic fluorescence titration curve was observed, confirming the previous observation reported by this laboratory (Heyduk and Lee (1989) *Biochemistry 28*, 6914−6924). However, the triphasic titration curve obtained from the ITC study suggests that the cAMP binding to CRP is more complicated than the previous conclusion that CRP binds sequentially two molecules of cAMP with negative cooperativity. The binding data can best be represented by a model for two identical interactive high-affinity sites and one low-affinity binding site. Unlike cAMP, the binding of cGMP to CRP exhibits no cooperativity between the high-affinity sites. The effects of mutations on the bindings of cAMP and cGMP to CRP were also investigated. The eight CRP mutants studied were K52N, D53H, S62F, T127L, G141Q, L148R, H159L, and K52N/H159L. These sites are located neither in the ligand binding site nor at the subunit interface. The binding was monitored by fluorescence. Although these mutations are at a variety of locations in CRP, the basic mechanism of CRP binding to cyclic nucleotides has not been affected. Two cyclic nucleotide molecules bind to the high-affinity sites of CRP. The cooperativity of cAMP binding is affected by mutation. It ranges from negative to positive cooperativity. The binding of cGMP shows none. With the exception of the T127L mutant, the free energy change for DNA−CRP complex formation increases linearly with increasing free energy change associated with the cooperativity of cAMP binding. This linear relationship implies that the protein molecule modulates the signal in the binding of cAMP, even though the mutation is not directly involved in cAMP or DNA binding. In addition, the significant differences in the amplitude of fluorescent signal indicate that the mutations also affect the surface characteristics of CRP. These results imply that these mutations are not perturbing specific pathways of signal transmission. Instead, these results are more consistent with the concept that CRP exists as an ensemble of native states, the distribution of which can be altered by these mutations.

The transcription of over 20 different operons encoding proteins involved in translocation and metabolism of carbohydrates in *Escherichia coli* is activated by the binding of adenosine 3′,5′-cyclic monophosphate (cAMP) receptor protein (CRP)[1] to the operons. CRP is a dimer of two identical subunits, each consisting of 209 amino acid (*1*, *2*). The crystal structure of the CRP−cAMP complex shows that each subunit is folded into two distinct functional and structural domains that are connected by a hinge region. The large N-terminal domain contains a long C-helix that is involved in extensive intersubunit contact and an extensive network of β-sheets forming the cAMP-binding pocket. The small C-terminal domain consists of the DNA-binding helix−turn−helix motif that makes base-specific contacts with CRP-dependent promoter (*3*, *4*).

CRP conformation and activity of CRP are dependent upon the binding of cAMP and the fluctuation in the concentration of cAMP. The mechanism of cAMP induced subunit−subunit and domain−domain communications remains a fundamental issue to the understanding of the regulatory mechanism of CRP. There are multiple cAMP binding sites in CRP. Occupancy of these sites seems to have differential effects on the affinity of CRP for specific DNA sites. Thus, an elucidation of the molecular mechanism of CRP function depends on a quantification of cAMP binding affinity and stoichiometry. Over the last two decades, cAMP binding had been analyzed using a variety of methods, including fluorescence assay, equilibrium dialysis, radioactivity assay, protease digestion, and so on. Results of these studies can best be described as the binding of two molecules of cAMP with the apparent dissociation constants ranging from 10^{-5} to 10^{-3} M. The binding of the first leads to a weaker affinity for the second ligand i.e., negative cooperativity between

† Supported by NIH Grant GM45579 and Robert A. Welch Foundation Grants H-0013 and H-1238.

* To whom correspondence should be addressed. Phone: (409) 772-4298. Fax: (409) 772-4298. E-mail: jclee@utmb.edu.

[1] Abbreviations: ANS, 8-anilino-1-naphthalene sulfonic acid; cAMP, adenosine 3′,5′-cyclic monophosphate; cGMP, guanosine 3′,5′-cyclic monophosphate; cNMP, nucleotide 3′,5′-cyclic monophosphate; CRP, cAMP receptor protein; TEK(X), 50 mM Tris, X mM KCl, 1 mM EDTA at pH 7.8, where X = 100, 200, or 500; ITC, isothermal titration calorimetry; H/D exchange, hydrogen−deuterium exchange.

10.1021/bi026099z CCC: $22.00
Published on Web 09/07/2002

sites (*5*, *6*), although Takahashi et al. reported that the cooperativity can change from positive to negative as a function of salt concentration (*7*, *8*). The crystal structure of CRP, solved initially at 2.9 Å resolution (*9*), later refined to 2.5 Å (*3*), and the structure of CRP complexed with cAMP and DNA (*4*, *10*) confirmed the stoichiometry of 2 cAMP per CRP dimer. Nevertheless, contradictory results with respect to cAMP binding to CRP were found scattering in the literature. cAMP in the anti conformation was observed in the crystal structure, whereas cAMP in the syn conformation was reported in NMR study (*11*). Gorshkova et al. reported that CRP is saturated with two cAMP molecules in 0.6 mM cAMP with ITC study (*12*). This report differs from the results which show that the second cAMP binding affinity is in millimolar range. In 1997, Passner and Steitz found additional cAMP molecules in the crystal structure of CRP complexed with cAMP and DNA (*13*). One pair of ligands with the anti conformation are located in the *N*-terminal domain and the other pair of ligands with the syn conformation at the interface between the N- and C-terminal domains, with contributions in part by residues of both subunits of CRP dimer. The binding of cAMP with the syn conformation was recently observed in the crystal structure of cAMP-liganded T127L/S128A double mutant CRP (*14*). This ligand was located at the surface of the C-terminal domain of the closed subunit. These reports have clarified the discrepancy between the NMR and crystallography studies; namely, the conformation of the bound cAMP is dependent on the site to which the cAMP is bound. Other important issues nevertheless remain to be addressed: what are the binding affinities of cAMP to these sites in CRP? Which conformation is the active form and binds DNA specifically? Does CRP−$(cAMP)_4$ or DNA−CRP−$(cAMP)_4$ exist in solution? If yes, does it imply any biological significance? It is imperative that the stoichiometry and potential cooperativity of cAMP binding to CRP be defined definitively.

Binding of cAMP induces conformational changes in CRP, enabling it to recognize specific DNA sequence. This is accomplished through long-range communications. Identification of structural elements in CRP responsible for transmitting information from subunit to subunit and from domain to domain is a key factor in understanding how this long-range communication is accomplished in CRP. Thus, cyclic nucleotide binding studies were conducted with eight CRP mutants (K52N, D53H, S62F, T127L, G141Q, L148R, H159L, K52N/H159L) which were chosen to disturb the thermodynamic linkage in the ligand binding processes. The determination of the perturbation of site−site communication in cyclic nucleotide binding allows one to address the role of subunit−subunit interaction in the mechanism of allosteric activation of CRP. Finally, the binding affinity to lac DNA and the energetics of site−site communication were correlated to elucidate the functional linkage between these two phenomena.

MATERIALS AND METHODS

Materials. Magnesium salt of 8-anilino-1-naphthalene sulfonic acid (ANS) was a product of INC Biochemical (Aurora, OH). cAMP and cGMP were purchased from Sigma (Saint Louis, MO). Phenyl sepharose was a product of Amersham Pharmacia Biotech (Uppsala Sweden). All other reagents were the highest grade commercially available.

Scheme 1

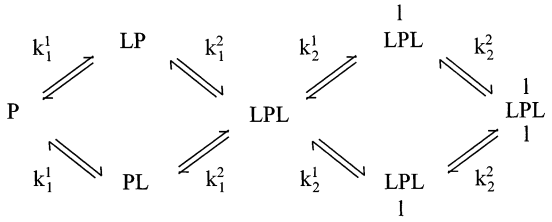

P:CRP L: high affinity cAMP site l: low affinity cAMP site

Methods. The concentrations of protein, cyclic nucleotide, and fluorescence probe were determined by absorption spectroscopy using the following absorption coefficients: 40 800 $M^{-1}cm^{-1}$ at 278 nm for CRP dimer (*6*); 14 650 $M^{-1}cm^{-1}$ at 259 nm and 12 950 $M^{-1}cm^{-1}$ at 254 nm for cAMP and cGMP (*15*), respectively; 6420 M^{-1} cm^{-1} at 351 nm for ANS (*16*). Absorption spectra were measured using a Hitachi U-2000 spectrophotometer.

Protein Purification. Site-direction mutagenesis of CRP mutants was constructed as described (*17*). The WT and mutant CRPs were purified from *E. coli* strains K12 Δ*H*1 and CA8445/pPRK248cI^{ts} using a previously described protocol (*5*). In addition, phenyl sepharose column was applied to remove low molecular weight impurity. Protein purified with this added step showed significant enhancement in DNA binding affinity and much less tendency to aggregate. The purified CRPs were >99% homogeneous, as judged by SDS-polyacrylamide gel electrophoresis with a loading of 50−60 μg/lane. The ratio of absorbance at 280 nm to that at 260 nm was larger than 1.86. This result indicated that contaminated DNA was removed. Protein mass was further checked with mass spectrometry. CRP was stored at −20 °C in the buffer containing 50 mM phosphate, 1 mM K_2EDTA, 1 mM DTT, 100 mM KCl, and 10% glycerol at pH 7.5. Under this condition, WT and mutant CRP were stable for up to 12 months of storage without a decrease in DNA binding affinity. However, the L148R mutant generally loses DNA binding affinity after 2−3 weeks of storage. Hence, experiments that involved L148R mutant were carried out only with freshly purified protein. Protein was routinely dialyzed against the described buffer and gently filtered through a membrane with a pore size of 0.22 μm before being used.

Reaction Mechanism. A four-cyclic-nucleotide binding site model was used to described the binding reaction between cAMP and CRP. The reaction mechanism is shown in Scheme 1 with microscopic association constants, $k^1{}_1$ and $k^2{}_1$ for the high-affinity binding sites and $k^1{}_2$ and $k^2{}_2$ for the low-affinity binding sites.

Ligand Binding Monitored by Fluorescence. All fluorescence experiments were conducted in buffer TEK(100) at 25 °C. Ligand binding to CRP was measured by the quenching of the fluorescent signal from the ANS−CRP complex. The basic protocol and instrumentation employed have been described previously (*5*, *18*) with minor modification. Decay of light intensity from excitation source during the long titration procedure could lead to misleading fluorescence signal; thus, the ratio mode was used to correct for lamp and instrument stability. The quantum counter, rhodamine B in ethylene glycol (3 g/L), was placed in the reference channel of the spectrofluorometer. The excitation

and emission wavelengths were 350 and 480 nm, respectively. Fluorescence data were collected with excitation and emission polarizers set at "magic angles" to eliminate polarization effects (*19*). The temperature of the cuvette holder was regulated with circulating water set at 25 ± 0.1 °C, and quartz cells of 10 × 10 mm were used. CRP solution at 3−4 μM in the presence of 40−50 μM ANS was titrated with cAMP in TEK(100) at 25 °C. The stock solutions of ligands at 0.5−100 mM were prepared in TEK(100) with pH readjusted to 7.8. All fluorescence signals were corrected for dilution. Before the observed data were analyzed, a few control experiments were included. Details are described in Results.

Cyclic nucleotide binding data obtained from fluorescence in this study were fitted to the following equation by a Levenber-Marquardt fitting routine provided by Sigamaplot for window version 5.0 to yield the thermodynamic parameters k^i_i:

$$F_{obs} = \sum_{i=0}^{i} \chi_i F_i \quad (1)$$

where F_{obs} and F_i are values of the measured property and fluorescent property of CRP with different number of cAMP bound, respectively. On the basis of Scheme 1, χ_i is the fraction of CRP with different numbers of cAMP bound and can be described as follows:

$$\chi_i = \frac{\alpha_i}{\sum_{i=0}^{i} \alpha_i} \quad (2)$$

where the parameter, α_i, along with the corresponding number of cAMP bound is listed below with [L] as the free cAMP concentration

I	α_i
0	1
1	$2k^1{}_1[L]$
2	$k^1{}_1k^2{}_1[L]^2$
3	$2k^1{}_1k^2{}_1k^1{}_2[L]^3$
4	$k^1{}_1k^2{}_1k^1{}_2k^2{}_2[L]^4$

Ligand Binding Monitored by ITC. All the calorimetric experiments were performed in the TEK(200) at 25 °C, unless otherwise specified, to minimize aggregation of the protein−ligand complex. Titrations were carried out on the VP-ITC MicroCalorimeter (MicroCal, Inc., Northampton, MA), which was calibrated with electrically generated heat pulses as recommended by the manufacturer. All solutions were thoroughly degassed by stirring under vacuum for five minutes before using. Right after degassing, the concentration of protein and that of titrant were measured to eliminate the potential change in concentration during the degassing process. Ligands (cAMP, cGMP) were prepared in dialysate of the protein solution to minimize artifacts due to minor differences in buffer composition. Even though the buffer was 50 mM Tris, its buffering capacity was not enough to maintain the pH at 7.8 in preparing cAMP solutions greater than 3 mM. Adjustment of pH was needed. The pH of another aliquot of the buffer dialysate was adjusted to pH 10.0 with 10 M KOH. This solution was then used to adjust the pH of the ligand solution to 7.8. In most cases, the pH differences between buffer and ligand were less than 0.05 pH unit. The reaction cell contained 1.4372 mL of protein in buffer, and the reference cell contained water only. The injection syringe was filled with ligand solution and was rotating at 470 rpm during temperature equilibration and experiment. A titration experiment consisted of 40 injections. The first injection was 2 μL, and the subsequent 23 injections were 4 μL each. They were followed by 15 injections of 10 μL each. Injection speed was 0.5 μL/s with a 4 min interval between injections. A separate titration of the ligand solution into the buffer was performed to determine the heat of dilution of the ligand which was then subtracted from the heat obtained during the titration of the ligand solution into the protein solution.

Leverber-Marquardt algorithm performed by Microcal Origin scientific plotting software was used to fit the incremental heat of the ith titration ($\Delta Q(i)$) of the total heat, Q_t

$$\Delta Q(i) = Q(i) + \frac{dV_i}{V_0}\left[\frac{Q(i) + Q(i-1)}{2}\right] - Q(i-1) \quad (3)$$

where V_0 is the volume of the sample solution. For a two sequential binding model

$$Q_t = [P]_t V_0 \left[\frac{K_1{}^1[L]\cdot\Delta H_1}{1 + K_1{}^1[L] + K_1{}^1K_1{}^2[L]^2} + \frac{K_1{}^1K_1{}^2[L]^2\cdot(\Delta H_1 + \Delta H_2)}{1 + K_1{}^1[L] + K_1{}^1K_1{}^2[L]^2}\right] \quad (4)$$

where $[P]_t$ is the total CRP dimer concentration in the sample

$$[L] = [L]_t - \left[\frac{[P]_t\cdot K_1{}^1[L]}{1 + K_1{}^1[L] + K_1{}^1K_1{}^2[L]^2} + \frac{2\cdot[P]_t\cdot K_1{}^1[L]^2}{1 + K_1{}^1[L] + K_1{}^1K_1{}^2[L]^2}\right] \quad (5)$$

vessel, $[L]_t$ is the total ligand concentration, ΔH_i's are the binding enthalpies, and $K^i{}_1$'s are the macroscopic binding constants for the high-affinity binding sites. $K^1{}_1$ and $K^2{}_1$ correspond to microscopic binding constants $2k^1{}_1$ and $^1/_2k^2{}_1$ (Scheme 1), respectively. For the model of a single set of identical independent site

$$Q_t = \frac{n[P]_t\Delta H V_0}{2}\left[1 + \frac{[L]_t}{n[P]_t} + \frac{1}{nK[P]_t} - \sqrt{\left(1 + \frac{[L]_t}{n[P]_t} + \frac{1}{nK[P]_t}\right)^2 - \frac{4[L]_t}{n[P]_t}}\right]$$

where n is the number of sites and K is the binding constant. Standard deviations for ΔH_i and $K^i{}_1$ from multiple titration runs were calculated.

RESULTS

Binding of cAMP. A. Monitored by ANS Fluorescence. cAMP binding to CRP was measured by monitoring the

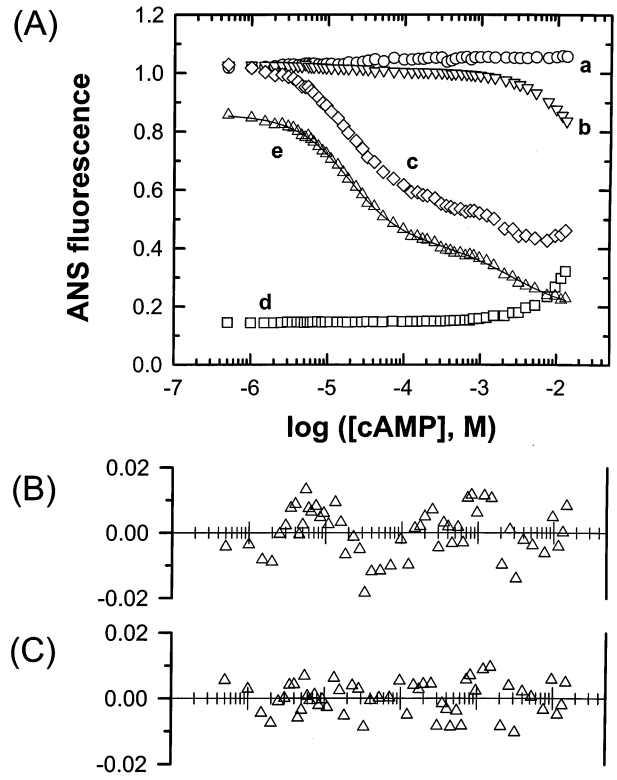

FIGURE 1: Binding of cAMP to CRP monitored by fluorescence quenching of CRP−ANS. The symbols representing fluorescence signal from cuvette A−D are as follows: ○, ▽, ◇, and □. Curve e and △ represent the corrected curve. Cuvettes A−C contained 3.6 μM CRP and 47.7 μM ANS in the TEK(100) at 25 °C. Cuvette D contained the same concentration of ANS but without protein. During the binding assay, no buffer or ligand was added to cuvette A. Into cuvettes B and C were titrated the same volume of buffer and ligand, respectively. To cuvette D were titrated aliquots of ligand. All ANS fluorescence reported here was corrected for dilution effect. Residuals are plotted as the observed values minus the calculated values according to eq 1 with constraints (B) $i = 2$ and (C) $i = 3$. The recovered parameters are summarized in the Table 1.

quenching of ANS−CRP fluorescence. It has been shown previously that ANS binds to CRP noncovalently and that the binding of cAMP leads to a dissociation of ANS from the CRP−ANS complex. As a consequence, a decrease in the ANS fluorescence signal was observed (*5*). The method is highly sensitive to perturbations. A few control experiments were included to address the issues on (a) photobleaching, (b) dilution, and (c) the effects of high concentrations of cAMP. In practice, four cuvettes were employed simultaneously in each titration experiment. Photobleaching of sample during the long titration procedure could lead to misleading fluorescence signal. Thus, the emission intensity of a CRP−ANS solution in cuvette A was monitored at the beginning of each addition of cAMP. As shown in Figure 1A, curve a, the fluorescence signal of ANS was stable for the total duration of the titration process. This result indicated that no photobleaching has occurred. The addition of each aliquot of cAMP resulted in a dilution of the CRP−ANS solution. Dilution decreases probe concentration and consequently reduces the inner filter effect. Additionally, the dilution might perturb the equilibrium and decrease fluorescence signal as a result of ANS dissociation. Thus, the emission intensity of a CRP−ANS solution in cuvette B was monitored with each additional aliquot of buffer. As shown in Figure 1A, curve b, the fluorescence signal began to decrease with addition of buffer, the amount of which was equivalent to the addition of 10^{-5} M cAMP and the change was quite significant at volumes equivalent to $>10^{-3}$ M cAMP. The magnitude of change was a function of protein; namely, in the presence of a different CRP mutant, the shape of the curve might be different. In cuvette C, the CRP−ANS solution was titrated with aliquots of a concentrated solution of cAMP. As shown in Figure 1A, curve c, the observed titration curve is at least biphasic. The effect of cAMP, especially at high ligand concentration, on ANS fluorescence was monitored in cuvette D. As shown in Figure 1A, curve d, the fluorescence signal of free ANS increased significantly when the concentration of cAMP was greater than 10^{-3} M. Increase in ionic strength or pH change would not lead to an increase in signal. As a consequence of these effects on the observed fluorescence intensity, the actual signal for cAMP binding, F, was obtained in accordance to

$$F = \left(\frac{F_c}{F_b}\right) - F_d \qquad (7)$$

where F_c, F_b, and F_d are the observed signal in cuvettes c, b, and d, respectively. Figure 1A, curve e, shows the corrected titration curve for cAMP binding to CRP. The resultant of these corrections was a titration curve with better defined fine features, such as a clear second phase of cAMP binding at $>10^{-3}$ M cAMP. The binding event can be very reliably reflected by the change in fluorescence signal at $<10^{-3}$ M cAMP. Even at cAMP concentrations $>10^{-3}$ M, with appropriate attention to experimental details, valid data can be acquired.

The binding of cAMP to CRP, as shown in Figure 1A, curve e, exhibited a biphasic pattern, an observation that is consistent with previous result from this lab (*5*). The initial phase occurred in micro-molar concentration range (0−500 μM cAMP), while the second phase occurred in the millimolar concentration range (1−20 mM cAMP). The association constant for the binding of cAMP was determined by fitting the observed data to eq 1. First the data were fitted for a model with two sites, i.e., $i = 2$, the same as that described by Heyduk and Lee (*5*). This simple two-site model fits the binding isotherm moderately well, as evidenced by the reasonably random distribution of residuals (Figure 1B). The recovered parameters summarized in Table 1 are in good agreement with the reported result (*5*). Nevertheless, when it was set for $i = 3$ (i.e., three sites, two high-affinity and one low-affinity binding sites), the fitting improved significantly, as indicated by the improvement in the random distribution of the residuals (Figure 1C). When $i = 4$ was set, the fitting did not improve (data not shown), or a physically meaningless negative value for k^2_2 was recovered. Scheme 1 may still be a valid model, even though only three microscopic association constants are needed to describe the titration isotherm. One possible reason may be that the observed amplitude for cAMP binding to the low-affinity sites is too small to be accurately measured. Another possibility is that the two low-affinity sites exhibit a strong negative cooperativity, resulting in great difficulty in obtaining an accurate estimation of the association constant for k^2_2 by direct binding experiments.

Table 1: Association Constants of CAMP and CGMP Binding to CRP Derived from ANS−CRP Fluorescence Titration

cAMP

two sites, $i = 2$		three sites, $i = 3$	
k^1_1 (10^4 M^{-1})	2.64 ± 0.01	k^1_1 (10^4 M^{-1})	3.2 ± 0.6
		k^2_1 (10^4 M^{-1})	6 ± 2
k^1_2 (10^4 M^{-1})	0.034 ± 0.001	k^1_2 (10^4 M^{-1})	0.011 ± 0.001
F_0	0.876 ± 0.003	F_0	0.861 ± 0.003
F_1	0.392 ± 0.005	F_1	0.655 ± 0.091
F_2	0.167 ± 0.013	F_2	0.413 ± 0.006
		F_3	0.182 ± 0.007

cGMP

model	negative cooperativity, $i = 1$	identical independent, $i = 2$	
constraints	$k^2_1 = 0$	$k^1_1{}^a = k^2_1$	$k^1_1 = k^2_1$ and $F_1 = F_2$
k^1_1 (10^4 M^{-1})	2.25 ± 0.01	4.5 ± 167.2	1.97 ± 0.01
F_0	0.994 ± 0.002	0.994 ± 0.003	0.983 ± 0.003
F_1	0.441 ± 0.002	0.72 ± 10.30	0.473 ± 0.003
F_2		0.441 ± 0.003	

[a] Equivalent sites.

B. Monitored by Anisotropy of DNA−CRP Complex Formation. The binding affinity of CRP with DNA is a function of cAMP concentration, as monitored by fluorescence anisotropy (*17*, *18*, *20*, *21*). The signal increased with increasing cAMP concentration, reached a plateau, and then the signal decreased. This bell shape behavior implies that different CRP−cAMP species are present and they recognize specific DNA site with different affinities. This bell shape behavior, as shown in Figure 2, was employed to assist in defining the stoichiometry of cAMP binding site. If CRP has two cAMP binding sites, then CRP can exist in three conformers, namely, free protein (P), singly liganded (PL), and doubly liganded protein (PL_2). On the basis of the fitting data listed in Table 1, the fraction of CRP conformers as a function of cAMP concentration was calculated. The distribution of the PL conformer (solid line) became significant at 10 μM cAMP and reached a maximum at 200 μM of cAMP. Concurrently, the fraction of PL_2 (dashed line) increased when the concentration of cAMP was > 200 μM, as shown in Figure 2, upper panel. This pattern of the distribution of CRP conformers could qualitatively fit the bell shape observation of fluorescence anisotropy as a function of concentration of cAMP if one assumes that the PL_2 conformer has significantly weaker affinity for DNA than PL. Thus, a two-site model can describe the observed DNA binding data. However, if CRP has four cAMP binding sites it can exist in five conformers, P, PL, PL_2, PL_2I, and PL_2I_2. Assuming that the magnitude of fluorescence anisotropy reflects the concentration of DNA−CRP complex regardless of the number of cAMP bound, the fraction of the PL conformer (solid line) increased with increasing concentration of cAMP and reached a maximum at 20 μM of cAMP and then decreased with further increase in cAMP concentration. In a parallel fashion PL_2 (dashed line) increased and reached a maximum at 300 μM, as shown in Figure 2, lower panel. At this concentration of cAMP the observed fluorescence anisotropy was also at a maximum value. The pattern of the distribution of the PL and PL_2 conformers was tracked by the increasing value of fluorescence anisotropy that monitors the formation of CRP−DNA complexes. The decreasing value of fluorescence anisotropy was tracked by the increasing fraction of PL_2I. Again, this pattern of distribution of CRP conformers could qualitatively fit the bell shape curve of the fluorescence anisotropy data, if one assumes that different CRP conformers exhibit different affinities for DNA. Thus, it can be concluded that the four-site model is as good as the two-site model to describe the interaction of DNA and CRP.

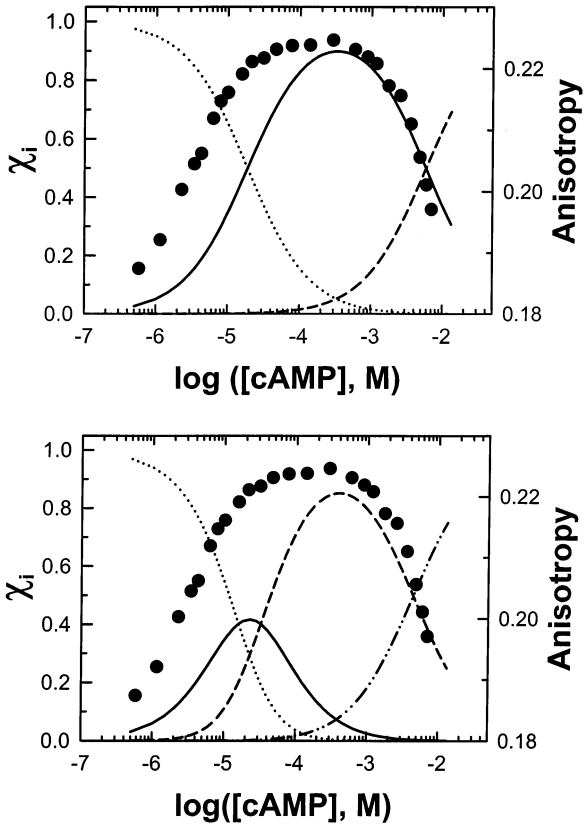

FIGURE 2: Simulation of CRP−cAMP conformers as a function of concentration of cAMP. The anisotropy data (•) were adopted from a previous study (*17*). On the basis of a model of 4 cAMP binding sites (Scheme 1), the fraction of each conformer (χ_i) was calculated with eq 1 and parameters listed in Table 1. The symbols and CRP species are as follows: (•••), P; (−), PL; (- -), PL_2; and (-•-), PL_2I, where P and L (l) are CRP and cAMP, respectively.

C. Monitored by ITC. Gorshkova et al. reported the observation of a biphasic titration isotherm for the binding interaction of cAMP to CRP (*12*). The initial binding reaction of cAMP to CRP was exothermic ($\Delta H < 0$) followed by an endothermic ($\Delta H > 0$) phase. This opposite phenomenon in heat exchange clearly indicated that the reaction of cAMP binding to CRP involves at least two types of binding sites. In this study, this biphasic observation was confirmed. However, the biphasic titration isotherm was achieved at a cAMP concentration below 1 mM. This cAMP concentration range is compatible with that associated with the initial phase of ANS−CRP titration, as shown in Figure 1, namely, within the range that the binding of cAMP to the strong sites was observed. The observed ITC data could only be fitted to the two-site sequential binding model, described by eq 3. The recovered thermodynamic parameters are listed in Table 2.

On the basis of the ITC study, the macroscopic association constants for cAMP binding to CRP were 8.0×10^4 and 3.5×10^4 M^{-1} which correspond to microscopic association constants of 4.0×10^4 and 6.9×10^4 M^{-1}, respectively.

Table 2: Recovered Parameters from ITC Studies

ligand	cAMP	cGMP		
model	two-sequential	two-sequential	one class	
N	2	2		1.99 ± 0.02
K^1_1[a] (10^4 M^{-1})	8 ± 1	8 ± 2	K (10^4 M^{-1})	4.2 ± 0.3
K^2_1[a] (10^4 M^{-1})	3.5 ± 0.5	2.1 ± 0.2		
ΔH_1 (cal/mol)	-2200 ± 100	-2800 ± 100	ΔH (cal/mol)	-2700 ± 80
ΔH_2 (cal/mol)	5500 ± 200	-2600 ± 100		
ΔS_1 (cal mol^{-1} K^{-1})	15 ± 1	12 ± 1	ΔS (cal mol^{-1} K^{-1})	12.1 ± 0.0
ΔS_2 (cal mol^{-1} K^{-1})	39.1 ± 0.3	11.1 ± 0.2		
K^1_1/K^2_1	2.3 ± 0.3	3.6 ± 0.4		

[a] K^1_1 and K^2_1 are macroscopic association constants, corresponding to microscopic association constants, $2k^1_1$ and $^1/_2k^2_1$.

These values are in excellent agreement with the results derived from the ANS−CRP fluorescence titration data, namely, $k^1_1 = 3.2 \times 10^4$ M^{-1} and $k^2_1 = 6.3 \times 10^4$ M^{-1} if the data were fitted to the three-site binding model (Table 1). Though the experiments were performed at different salt concentrations (fluorescence titration in TEK(100) and ITC in TEK(200)), this comparison is still valid since cAMP binding affinity at <0.2M salt is independent of salt (*8*).

The interaction of cAMP to the low-affinity site is very difficult to demonstrate with ITC because of the intensive heat of dilution of the ligand. A typical set of ITC data acquired in the buffer TEK(500) at 35°C is shown in Figure 3A. The observed heat change, involving both cAMP binding and ligand dilution, increased at the first five injections, reached a peak, sharply decreased, and finally slightly increased again with additional titrant. To quickly reach a higher concentration of cAMP and to make it easier to detect the heat exchange involved, the injection volume was increased after the high-affinity sites were occupied, as indicated by the arrow. The heat change of ligand dilution was large. As demonstrated in Figure 3B, which showed the results of a parallel control experiment with cAMP titrated into buffer, the heat of dilution assumed a magnitude similar to that of binding. The reaction heat change upon cAMP binding was then presented as the difference between these two titrations. The heat exchanged versus ratio of total ligand concentration to total protein concentration is shown in Figure 3C. The first binding reaction of cAMP to CRP was exothermic, and the second cAMP binding was strongly endothermic. The third cAMP binding was exothermic again. This may result in the overall endothermic and then exothermic nature of the total three-step binding reaction. All of the above results clearly illustrate that the binding of cAMP to CRP involves two high-affinity and at least one low-affinity binding processes.

D. Effect of Single Site Mutations on cAMP Binding. Seven single site mutants, K52N, D53H, S62F, T127L, G141Q, L148R, and H159L, and one double mutant K52N/H159L, which presumably disturb the thermodynamic linking equilibrium of cAMP binding, were used to investigate the structural elements which modulate inter- and intramolecular interactions. These mutation sites are not located in the ligand binding site or at the subunit interface. Residues 52, 53, and 62 are in a loop between β-3 and β-4. While residue 127 is in the C-helix, residues 141 and 148 are in the D-helix. Residue 159 is in β-7. Although ITC is capable of providing thermodynamic binding parameters directly, the application of this method is limited by protein solubility. Submillimolar range of protein concentration is required for ITC experiments to pursuit accurate estimation of binding parameters when cAMP binding association constant is as low as 10^4 M^{-1}. It is extremely difficult to prepare protein at such a high concentration for some CRP mutants. Thus, the binding processes were monitored by the quenching of CRP−ANS fluorescence upon cAMP binding (Figure 4). Similar to WT CRP, five mutants (D53H, G141Q, L148R, H159L, and K52N/H159L) exhibited biphasic binding isotherms. However, the binding isotherms for K52N, S62F, and T127L showed a single phase S-shaped curve up to 10 mM

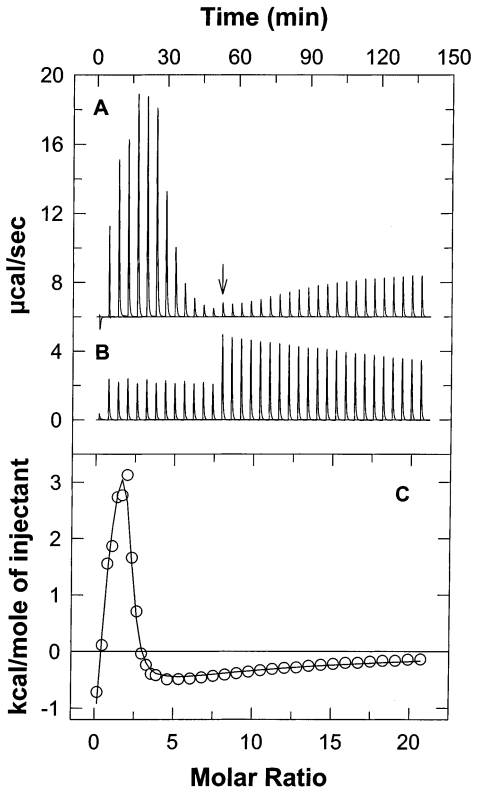

FIGURE 3: Demonstration of low-affinity cAMP binding site with ITC measurements. Titration was preformed in TEK (500) at pH 7.8 and 35 °C. (A) Calorimetric titration of a stock solution of 23.44 mM cAMP to a solution of 212.2 μM CRP. The titrating aliquots are as follows: 2 μL for the first injection, 4 μL each for the 2−13 injections, and the final 22 injections with 9 μL each. (B) In a parallel control experiment, 23.44 mM cAMP was added into buffer. (C) The heat exchanged upon addition of titrant vs the ratio of the total concentration of ligand to the total concentration of protein. The solid line represents the best fit of a model of sequential binding to three sites. The recovered parameters: $K^1_1 = (11.4 \pm 2.6) \times 10^4$ M^{-1}, $\Delta H_1 = -1522 \pm 266.9$ cal/mol, $\Delta S_1 = 18.2$ cal mol^{-1} K^{-1}, $K^2_1 = (5.8 \pm 1.5) \times 10^4$ M^{-1}, $\Delta H_2 = 7049 \pm 348.6$ cal/mol, $\Delta S_2 = 44.68$ cal mol^{-1} K^{-1}, $K^1_2 = 229 \pm 102$ M^{-1}, $\Delta H_3 = -15110 \pm 4011$ cal/mol, $\Delta S_3 = -38.22$ cal mol^{-1} K^{-1}.

Table 3: Recovered Parameters for Cyclic Nucleotide Binding[a]

	cAMP				cGMP
	k_1^1 ($\times 10^4$ M^{-1})	k_1^1 ($\times 10^4$ M^{-1})	k_1^1 ($\times 10^2$ M^{-1})	k_1^2/k_1^1	k_1 ($\times 10^4$ M^{-1})
WT	3.2 ± 0.6	6.2 ± 1.9	1.1 ± 0.1	1.96	1.97 ± 0.06
K52N	1.6 ± 0.2	0.35 ± 0.25		0.22	1.27 ± 0.04
D53H	2.1 ± 0.4	54.1 ± 16.1	2.4 ± 0.5	21.33	2.45 ± 0.09
S62F	0.19 ± 0.01	0.015 ± 0.005		0.08	0.193 ± 0.004
T127L	2.0 ± 0.3	0.6 ± 0.7		0.32	1.66 ± 0.04
G141Q	1.8 ± 0.3	12 ± 4	1.3 ± 0.3	6.67	1.93 ± 0.04
L148R	2.0 ± 0.4	130 ± 40	2.8 ± 0.4	55.8	2.50 ± 0.06
H159L	3.6 ± 0.3	5 ± 2	1.46 ± 0.08	1.15	2.27 ± 0.09
K52N/H159L	1.3 ± 0.1	0.2 ± 0.2	3.08 ± 0.08	0.17	1.22 ± 0.04

[a] $\pm$ denotes standard error from the fit. At least two titration were performed for all the mutants.

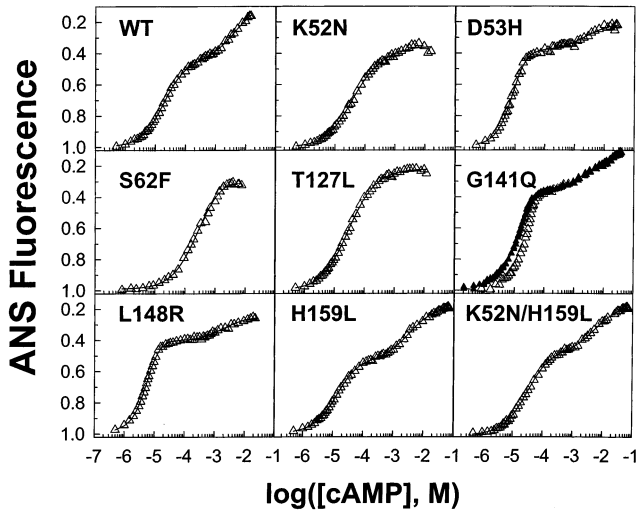

FIGURE 4: Binding of cAMP to CRP mutants as monitored by fluorescence quenching of CRP−ANS. Measurements were performed in TEK(100) at 7.8 and 25°C, with 3−4 μM CRP and 40−50 μM ANS, except G141Q due to its weak dimerization. The protein concentration was 20.0 μM, and ANS concentration was 70.0 μM for the G141Q titration. The binding isotherms of cAMP to D53H, G141Q, L148R, H159L, and double mutant K52N/H159L were best fitted to eq 1 under constraint $i = 3$. The binding data of cAMP to K52N, S62F, and T127L were analyzed with the constraint $i = 2$. Data analysis for G141Q was described in the text. The data points were normalized to that without ligand. The fitting results are shown as solid lines, and the recovered parameters are listed in Table 3.

concentration of cAMP. The initial phase of the titration curves for D53H and L148R were shifted to lower concentration of cAMP, decoupling the binding isotherm into two well defined phases. This shift suggested that the single substitutions of Asp53 to His and Leu148 to Arg increase CRP affinity for cAMP at the high-affinity binding sites. For WT, the initial phase of the binding isotherm spanned two log units of the concentration of cAMP to reach a saturation level covering from 10% to 90%, but this was narrowed down to one log unit for D53H and L148R. Therefore, a single site substitution of Asp 53 to His or Leu148 to Arg increases not only the cAMP binding affinity but also the cooperativity between the two high-affinity binding sites, as reflected by the steeper slope in the initial phase of the binding isotherm. In contrast, the titration curves for K52N, S62F, and T127L were shifted to higher concentrations of cAMP and spanned three log units of the concentration of cAMP in order to reach a saturation level from 10 % to 90%. One explanation is that single site substitutions of Lys52 to Asn, Ser62 to Phe, and Thr127 to Leu may lead to a decrease in the cAMP binding affinity of the strong sites, and consequently the two phases are merged into one S-shaped curve. Alternatively, mutations at these locations may switch the site−site communication between the two high-affinity sites into negative cooperativity and this methodology is not capable of resolving these low-affinity sites. In other words, this fluorescence approach is not able to detect cAMP binding to the low-affinity site since the signal is too small. Among the mutants being studied, H159L and K52N/H159L did not significantly change the shape of the cAMP binding isotherm, except that the amplitude for ANS quenching was different.

A model with two high-affinity sites and one low-affinity site was used to describe the interaction of CRP with cAMP. All titration curves, as shown in Figure 4, were fitted to eq 1 with constraint $i = 3$ for WT, D53H, S62F, G141Q, L148R, H159L, and K52N/H159L. The binding isotherms for mutants K52N, S62F, and T127L were fitted with constraint $i = 2$. When constraint $i = 3$ was set to fit the fluorescence data for K52N, S62F, and T127L, the fitting did not improve and a physically meaningless negative value for some of the parameters was recovered. The fitting results are shown as solid lines in Figure 4 and the recovered parameters are listed in Table 3. Similar to the WT CRP, the values of the association constants for cAMP binding to D53H CRP at strong binding sites are in excellent agreement with those determined by ITC[2].

The protein concentration of G141Q was 20.0 μM to ensure that CRP dimer was the dominant species being investigated. This is due to the weak dimerization constant for this mutant (*22*). With such a high concentration of protein, it is not valid to assume that the total cAMP concentration is the free cAMP concentration. Therefore, eq 1, in combination with an iterative routine, was used to estimate the cAMP binding association constants. First, the data were analyzed under the assumption that total cAMP concentration was equivalent to the free cAMP concentration. After obtaining the initial association constants, the free cAMP concentration was calculated accordingly. Then the data were reanalyzed with the calculated free cAMP concentration. This cycle was repeated until the fitting parameters did not change. In Figure 4, the filled symbols in the titration curve for G141Q represent the free cAMP concentrations after three iterative cycles.

Binding of cGMP. A. Monitored by ANS Fluorescence. Fluorescence quenching experiment with ANS as a probe was also used to monitor cGMP binding. The viscosity was high for the solutions containing high concentration of

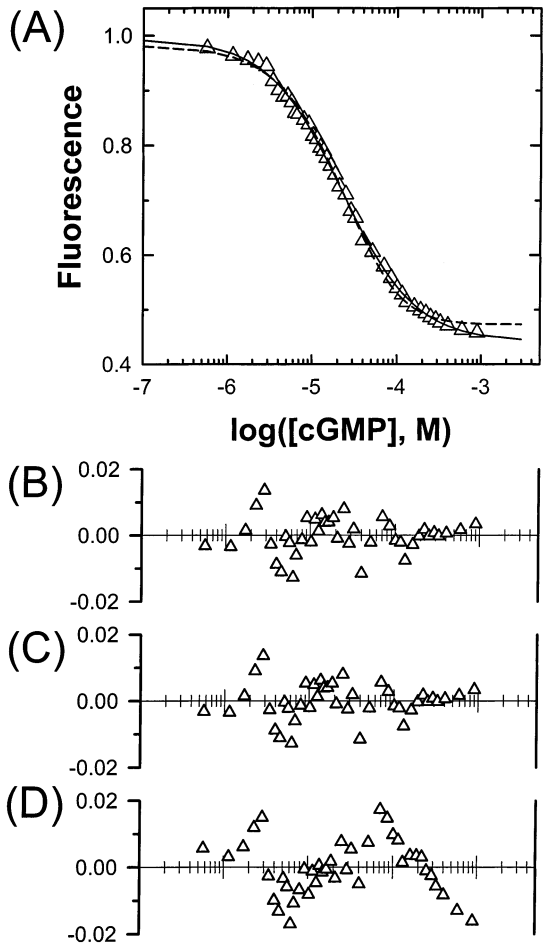

FIGURE 5: Binding of cGMP to CRP monitored by fluorescence quenching of CRP−ANS. (A) Measurement was performed in TEK(100) at pH 7.8 and 25 °C, with 3.7 μM CRP and 47.7 μM ANS. The two super imposed solid lines represent the best fit of the following models: one site and two identical independent sites with $F_1 \neq F_2$. The dashed line reflects the fitting result to a model of two identical independent sites with $F_1 = F_2$. The recovered parameters are summarized in Table 1. Residuals are plotted as the observed values minus the calculated values according to eq 1 in (B) $i = 1$, (C) $i = 2$, $k^1_1 = k^2_1$, and (D) $i = 2$, $k^1_1 = k^2_1$, and $F_1 = F_2$.

cGMP. Data obtained at high concentrations of cGMP became unreliable. Therefore, only the initial phase of the data was analyzed, even though biphasic titration curved was still observed (the 2nd phase data were not shown). Three sets of different constraint for eq 1 were used to define the stoichiometry of the high-affinity binding of cGMP to CRP. These were (1) a complete negative cooperative model, i.e., only one cGMP molecule could bind to one CRP dimer, (2) two-identical-independent site models, and (3) two-identical-independent site models with a $F_1 = F_2$ constraint, i.e., fluorescence signal for the CRP−cGMP complex formation is identical to that for CRP−$cGMP_2$. The purpose for the $F_1 = F_2$ constraint was to decrease the number of parameters for the fitting. The fitting results are shown in Figure 5A and the corresponding residues are plotted in panels B−D, respectively. In Figure 5A, the solid line represents the results from fitting to models 1 and 2. The experimental data could not distinguish between these two models since the two lines overlapped and the patterns for the distribution of residuals are identical, as shown in Figure 5B,C. However, a closer examination of the recovered parameters showed that k_1^1 and F_1 are very poorly defined as indicated by unacceptably large deviations. Thus, model 2 was discarded. Since there are two high-affinity sites for cAMP and there is no independent evidence to indicate that cGMP binds with a high degree of negative cooperativity, model 1 was dismissed. The dashed line represents the result from the fitting to model 3. The fit for this model is clearly not as good as indicated by the nonrandomness in the distribution of residuals, as shown in Figure 5D. Nevertheless, model 3 is physically a more reasonable model. Thus, the recovered parameters are accepted and listed in Table 1. The two-site sequential binding model is not shown since more parameters have to be introduced. In summary, data obtained from fluorescence study could not provide enough information to distinguish these models. The current result demonstrates that fluorescence titration provides information regarding the number of classes of ligand binding sites but does not necessarily provide information about the number of binding sites in each class.

B. Monitored by ITC. ITC was used to resolve the number of cGMP binding site to CRP. One binding site model could not describe the observation (Table 2), with recovered parameters $K = (0.52 \pm 0.08) \times 10^4$ M^{-1}, $\Delta H = -7266 \pm 481$ cal/mol, and $\Delta S = 17.1$ cal mol^{-1} K^{-1}. The observed ITC data could be well fitted to the two-site sequential binding model. The recovered parameters are listed in Table 2. The two macroscopic association constants were $K^1_1 = (8 \pm 2) \times 10^4$ M^{-1} and $K^2_1 = (2.1 \pm 0.2) \times 10^4$ M^{-1}, respectively. The ratio of these two constants was 3.6 ± 0.4. It approaches 4.0 and implies that these two sites in CRP are identical and independent with respect to cGMP binding. Furthermore, the ITC observation was fitted to a model of a single set of identical independent sites. As shown in Table 2, the number of binding site was 1.99 ± 0.02. Thus, data analysis shows that cGMP binds to the two subunits of CPR in an independent manner. In addition, contrary to the binding of cAMP to CRP, the cGMP binding reaction was exothermic for both sites. This observation is consistent with the report by Gorshkova et al. (*12*).

C. Effect of Single Site Mutations on cGMP Binding. The interactions between CRP mutants and cGMP were monitored by CRP−ANS fluorescence quenching (data not shown). The binding, with the exception of the S62F mutant, was studied up to a cGMP concentration of 1 mM because the solution became viscous and the titration was difficult to continue beyond 1 mM. Among the mutants studied, only the titration curve of S62F was shifted to the higher concentration of cGMP, implying a weaker binding affinity for cGMP. Amplitude, rather than the shape of titration curve, was significantly disturbed by the mutations. This observation implies that mutations affect the local environments of the ANS binding sites. It is interesting that all the titration curves spanned about two log units of the concentration of cGMP. This implies that the mutants do not affect the cooperativity of cGMP binding; in other words, cGMP binds independently to the two CRP subunits.

Consistent with result for WT CRP, all the cGMP binding data could be fitted to a model of two-identical-independent site, with $F_1 = F_2$, i.e., single and double liganded cGMP−CRP elicited the same magnitude of ANS fluorescence signal. The recovered parameters are listed in Table 3.

DISCUSSION

In discussing the issues of stoichiometry and cooperativity of ligand binding to CRP, one must be cognizant of the different regimes of ligand concentration in which these studies were conducted. The reports by most groups are limited to ligand concentrations below 1 mM (*7*, *8*, *12*), while the others are extended to 10 mM (*5*, *6*). The current study shows that CRP has two high-affinity and at least one low-affinity cAMP sites. This conclusion is based on the combined results of two independent methods, ITC and fluorescence (Figures 1, 3, and 4). The fluorescence titration data exhibit a biphasic pattern, confirming the results of the previous report (*5*). This biphasic pattern indicates the presence of two classes of cyclic nucleotide binding sites, namely, the high- and low-affinity sites (Figure 1). Within the current experimental conditions and within the constraints of the functional behavior of WT CRP, the fluorescence data cannot differentiate between a stoichiometry of 1 or 2 in each class. In the initial phase of the fluorescence titration curve (Figure 1), it is evident that it required a cAMP concentration range that spans about two log units to describe the occupancy of the site(s) between 10% and 90% level of saturation. This is an expected observation for a binding reaction that is not thermodynamically linked, e.g., communication between sites. In this case, the methodology cannot aid in defining the number of sites. However, if there were communication between sites, then the range of cAMP concentration required to reach 10−90% saturation would deviate from the two log units observed in this study. It could be as small a range as one log unit as observed in some CRP mutants, as shown in Figure 4. Although the fluorescence data for WT CRP do not provide enough information to independently define the number of sites in this initial phase of cAMP binding, the ITC data provide a clear indication of the presence of two binding events (Table 2). This is due to the significant differences in the thermodynamic signatures of cAMP binding to the two sites. One is characterized by an exothermic event while the other is endothermic. Thus, a combination of data from both approaches led to a definitive assignment of two binding events in this initial phase of cAMP binding. Consequently, consistent quantitative parameters were derived from both approaches, namely, two interactive sites which exhibit positive cooperativity with binding constants within the range of 3×10^4 to 6×10^5 M^{-1}.

Titration of CRP with cAMP to concentrations exceeding 1 mM led to the observation of the second phase in the fluorescence data (Figure 1). This represents the binding of cAMP to the weak sites, most likely as in the model presented by Passner and Steitz (*13*). The detection of this weak binding event is exactly the same as that reported by Heyduk and Lee (*5*) and can only be detected when the titration is extended to a cAMP concentration as high as 10 mM. It is reasonable that this weak binding event was not detected by the other studies which limited their titration to a cAMP concentration of less than 1 mM. Technically it is very difficult to measure such weak binding with equilibrium dialysis. It is equally challenging with ITC. A measurement of affinity as low as 10^4 M^{-1} in CRP necessitates the employment of high protein concentration for acquiring reliable heat exchange signal. Protein aggregation of CRP or CRP−cAMP complex leads to complicated signals that are difficult to resolve. In addition, the large heat exchange due to the heat of dilution of ligand renders the study of the low-affinity sites very difficult (Figure 3). Nevertheless, in this study it is evident that a combination for these two approaches can provide information that is a more complete description of the events involving cAMP binding to CRP. It clarified the stoichiometry discrepancy between the solution and crystallography studies, namely, the stoichiometry of 1:2 in solution studies (*5*−*8*, *12*) and 1:4 in CRP crystal structure (*13*, *14*).

Consistent with the data observed in WT CRP, biphasic CRP−ANS titration pattern for cAMP binding was observed with five CRP mutants, namely, D53H, G141Q, L148R, H159L, and K52N/H159L, supporting that CRP has two types of cAMP binding sites, namely, high-affinity and low-affinity cyclic nucleotide binding sites (Figure 4). There are at least two high-affinity cyclic nucleotide binding sites in a CRP molecule, as suggested by the observation that mutation of CRP could change the slope of the initial phase of the titration curve. Only one low-affinity cyclic nucleotide binding site was detected because cyclic nucleotide binds to the low-affinity sites with a strong, negative cooperativity. Although single phase CRP−ANS titration pattern was observed with K52N, S62F, and T127L, a three-site model has to be used to describe the cAMP binding to S62F with ITC study.[2] Since the four-site model is consistent with all the data for cAMP binding to WT and mutants, JCL is withdrawing the two-site model which was initially proposed for the WT CRP data (*5*).

The thermodynamic signatures of cAMP binding to the strong sites are very interesting. The binding to the first site is exothermic with a $\Delta H = -2.5$ kcal/mol (Table 2). In contrast, the occupancy of the second site is endothermic and the reaction is entropically driven. If one assumes that the increase in entropy is a reflection on the dynamics of the CRP molecule, then the net results of cAMP binding to these strong sites is an increase in the dynamic motion of CRP. Such an interpretation is in good agreement with the H/D exchange data which show that the amide protons in the α-helices of CRP exchange more rapidly in the presence of cAMP (*23*). In addition, this interpretation is in agreement with previous reports that the accessibility of Cys 178 in the DNA binding domain and suceptability to protease digestion increase with the occupancy of these high-affinity sites (*5*). As shown in Figure 2, CRP recognizes specific DNA sequence when both high-affinity sites are occupied by cAMP. In contrast, the binding of cAMP to the weak sites is characterized by a loss of entropy, i.e., $\Delta S_3 < 0$. If one continues to assume that this can be at least partially correlated to protein dynamics, then this result implies that the occupancy of these weak sites leads to a decrease in dynamics of CRP. Note that occupancy of these low-affinity sites also suppresses the affinity of CRP for specific DNA sequence (*5*, *17*, *20*, *21*). Thus, there seems to be a correlation between protein dynamics and affinity for DNA, namely, order and disorder with low and high affinity, respectively.

The interaction between cGMP with CRP seems to be quite different from cAMP. cGMP binds to the high-affinity

[2] Lin, S.-H., and Lee, J. C., manuscript in preparation.

sites with no signs of cooperativity. Binding of cGMP to the first site is still characterized as exothermic, and in contrast to the cAMP binding, subsequent binding of cGMP continues to be an exothermic reaction. Thus, binding of cGMP is not characterized by a significant increase in entropy. This observation is consistent with the H/D exchange data which indicate that cGMP does not induce the increase in proton exchange rate that is observed in the presence of cAMP (*23*). Hence, these thermodynamic signatures of ligand binding are revealing the activation mechanism of CRP by ligand binding.

Another important issue is the nature of communication among these binding sites and the consequences as reflected in the recognition of specific DNA sequences by CRP. Mutants, except S62F, do not affect the affinity for cyclic nucleotides, but they do significantly influence the site−site communication. The binding affinity for the first ligand ranged from 1.2×10^4 to 3.6×10^4 M^{-1} for cAMP and from 1.2×10^4 to 2.5×10^4 M^{-1} for cGMP (Table 3). This result suggests that CRP mutants investigated in the current study are able to recognize cGMP and cAMP to the same extent, and such recognition is not affected by the mutation. The binding affinity for the second ligand was dependent on the identity of the cyclic nucleotide occupying the first site. If the first site was occupied by cGMP, the affinity of the second site for cGMP appears to be the same as the first site, suggesting that the two high-affinity sites do not communicate with each other upon cGMP binding. However, if the first site was occupied with cAMP, then the second site affinity is dependent on the mutation. It could range from 6×10^3 M^{-1} to 1.3×10^6 M^{-1}. Although the side chains of the mutated amino acids, except T127L, do not have direct contact with cAMP, the cooperativity of cAMP binding was significantly affected by these single site amino acid substitutions. Knowledge of the coefficient of cooperativity (α), which is defined as the ratio of k_1^2/k_1^1, allows for the calculation of the change in free energy associated with the site−site interaction ($\Delta G(\alpha) = -RT \ln \alpha$), as summarized in Table 3. The cooperativity energy for cAMP binding is linearly correlated with the energetics of DNA binding, as shown in Figure 6. Therefore, the site−site (therefore subunit-subunit) communication in CRP determines the aptitude of CRP to recognize specific DNA sequence. The establishment of this linear correlation has a profound implication on the mechanism of DNA recognition by CRP. It implies that the CRP−cAMP and CRP−$cAMP_2$ species have different affinities for *lac* DNA. Furthermore, the CRP−$cAMP_2$ species should have a higher affinity for DNA than that of the mono-liganded CRP. On the basis of the results of this study, there are five possible conformers in CRP with different stages of bound cAMP. Does the presence of these conformers impact on the regulatory role of CRP? In an in vivo study, it was reported that only the complex formed at lower concentrations of cAMP is the transcriptionally active form for gal operon in *E.coli* (*24*). It implies that different cAMP responsive elements may exhibit a specific pattern of differential affinity toward these CRP conformers. Apparently, mutations in CRP can affect this pattern in their recognition of lac operon.[3]

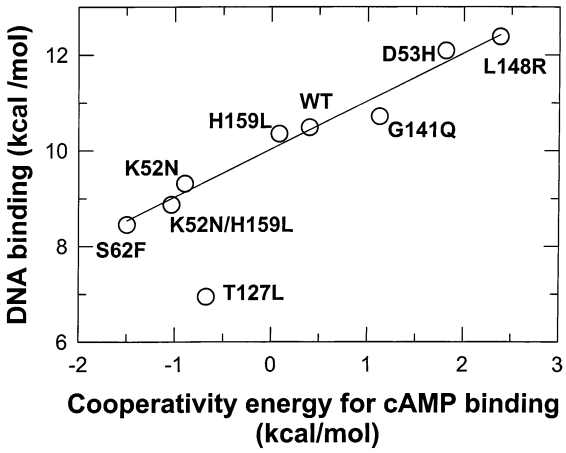

FIGURE 6: Correlation between the interaction energy of the two cAMP binding sites and the DNA binding affinity. The solid line represents the result of linear regression fit with slope = 1.00 ± 0.07 and intercept = 10.03 ± 0.09. DNA binding data were adapted from ref *17*, except the data for L148R and S62F. For L148R, the DNA binding study was performed with freshly purified protein. The affinity of DNA with S62F was estimated in the presence of 1 mM cAMP.

The issue of cooperativity between the two high-affinity sites is apparently quite complicated. Takahashi et al. (*7*) showed that CRP binds 2 molecules of cAMP. The interaction between these sites is characterized as negative cooperativity that is progressively changed to positive with increasing ionic strength. This study was conducted by equilibrium dialysis and the cAMP concentration was limited to less than 400 μM. The same authors reported that the binding affinity and cooperativity vary only slightly on salt concentration below 0.2 M (*8*), an observation consistent with this report (Tables 1 and 2). Gorshkova et al. (*12*) studied the interaction between CRP and cAMP by ITC. Their results indicated that CRP is capable of binding two molecules of cAMP. The binding exhibits features of positive cooperativity, the degree of which decreases with increasing ionic strength. This study was conducted with cAMP concentration limited to less than 600 μM. These reported difference in salt dependence may reflect an additional thermodynamic linkage to pH or other solution variables. This is an issue that is under active investigation.

Among the mutants studied, only S62F exhibits a diminished ability to bind cyclic nucleotides by about 10-fold (Table 3). Although Ser62 does not directly contact cAMP, its mutation is expected to sterically interfere with the binding of cAMP (*3*). The side chains of Ile60, Leu61, Tyr63, and Leu64 and the adenine moiety of cAMP form a ring that surrounds the side chain of Ser62. One side of the ring is solvent-accessible, and the other side is stacked with Ala48. The larger Phe side chain in the S62F mutant would impose an expansion on the surrounding ring structure and possibly affect the stability of the protein. Another possible effect of the mutation is that the larger Phe side chain could displace the adenine moiety of the bound cAMP from its preferred position. This displacement could result in a weakening of the binding of cAMP. The projected effects based on the proposed structural perturbation are consistent with the thermodynamic result from ITC study.[2]

[3] Lin, S.-H., and Lee, J. C., manuscript to be submitted.

[4] Kemmis, C., Lin, S.-H., and Lee, J. C., manuscript in preparation.

Besides the functional perturbations, mutations lead to an apparent global perturbation in the surface of CRP. The conclusion is derived from the observation that the change in the amplitude in ANS fluorescence was different with different mutants, implying that protein surface was disturbed by the single site mutation. This interpretation is supported by the changes in the interaction of these mutants with column matrixes during protein purification.[4]

Concluding Comment. Mutation at a variety of locations in CRP do not affect the basic mechanism of CRP. They do affect quantitatively the site−site communication and the surface characteristics of CRP. These results imply that these mutations are not perturbing specific pathways of signal transmission. Instead, these results are more consistent with the concept that CRP exists as an ensemble of native states, the distribution of which can be altered by these mutations.

REFERENCES

1. Aiba, H., Fujimoto S., and Ozaki N. (1982) *Nucleic Acids Res. 10*, 1345−1361.
2. Cossart P., and Gicquel-Sanzey B. (1982) *Nucleic Acids Res. 10*, 1363−1378.
3. Weber, I. T., and Steitz, T. A. (1987) *J. Mol. Biol. 198*, 311−326.
4. Parkinson, G., Wilson, C., Gunasekera, A., Ebright, Y. W., Ebright, R. H., and Berman, H. M. (1996) *J. Mol. Biol. 260*, 395−408.
5. Heyduk, T., and Lee, J. C. (1989) *Biochemistry 28*, 6914−6924.
6. Leu, S.-F., Baker, C. H., Lee, E. J., and Harman, J. G. (1999) *Biochemistry 38*, 6222−6230.
7. Takahashi, M., Blazy, B., and Baudras, A. (1980) *Biochemistry 19*, 5124−5130.
8. Takahashi, M., Blazy, B., Baudras, A., and Hillen, W. (1989) *J. Mol. Biol. 207*, 783−796.
9. McKay, D. B., Weber, I. T., and Steitz, T. A. (1982) *J. Biol. Chem. 257*, 9518−9524.
10. Schultz, S. C., Shields, G. C., and Steitz, T. A. (1991) *Science 253*, 1001−1007.
11. Gronenborn, A. M., Clore, G. M., Blazy, B., and Baudras, A. (1981) *FEBS Lett. 136*, 160−164.
12. Gorshkova, I. I., Moore, J. L., McKenney, K. H., and Schwarz, F. P. (1995) *J. Biol. Chem. 270*, 21679−21683.
13. Passner, J. M., and Steitz, T. A. (1997) *Proc. Natl. Acad. Sci. U.S.A. 94*, 2843−2847.
14. Chu, S. Y., Tordova, M., Gilliland, G. L., Gorshkova, I., Shi, Y., Wang, S., and Schwarz, F. P. (2001) *J. Biol. Chem. 276*, 11230−11236.
15. Merck & Co., Inc. (1976) in *The Merck Index*, 9th ed., p 353, Rahway, NJ.
16. Ferguson, R. N., Edelhoch, H., Saroff, H. A., and Robbins, J. (1975) *Biochemistry 14*, 282−290.
17. Lin, S.-H., Kovac, L., Chin, A. J., Chin, C. C. Q., and Lee, J. C. (2002) *Biochemistry 41*, 2946−2955.
18. Cheng, X. D., Kovac, L., and Lee, J. C. (1995) *Biochemistry 34*, 10816−10826.
19. Lakowicz, J. (1983) in *Principles of Fluorescence Spectroscopy*, Plenum Press, New York.
20. Heyduk, T., and Lee, J. C. (1990) *Proc. Natl. Acad. Sci. U.S.A. 87*, 1744−1748.
21. Pyles, E. A., and Lee, J. C. (1996) *Biochemistry 35*, 1162−1172.
22. Cheng, X. D., and Lee, J. C. (1998) *Biochemistry 37*, 51−60.
23. Dong, A., Malecki, J., Lee, L., Carpenter J. F., and Lee, J. C. (2002) *Biochemistry 41*, 6660−6667.
24. Mukhopadhyay, J., Sur, R., and Parrack, P. (1999) *FEBS Lett. 453*, 215−218.

BI026099Z